Proceedings of the Estonian Academy of Sciences
2025, **74**, 2, 170–174

https://doi.org/10.3176/proc.2025.2.16

www.eap.ee/proceedings
Estonian Academy Publishers

POWDER METALLURGY

RESEARCH ARTICLE

Received 3 February 2025
Accepted 18 March 2025
Available online 2 May 2025

Keywords:
titanium carbonitride, iron-bonded cermets, chromium addition, mechanical properties, sustainability

Corresponding author:
Tabeen Halawat Pampori
tabeen.pampori@taltech.ee

Citation:
Pampori, T. H., Kolnes, M., Juhani, K., Tarraste, M. and Kübarsepp, J. 2025. Effect of high chromium content additions in iron-bonded Ti(C,N) cermets: a hardness-toughness tradeoff. *Proceedings of the Estonian Academy of Sciences*, **74**(2), 170–174. https://doi.org/10.3176/proc.2025.2.16

Effect of high chromium content additions in iron-bonded Ti(C,N) cermets: a hardness-toughness tradeoff

Tabeen Halawat Pampori, Märt Kolnes, Kristjan Juhani, Marek Tarraste and Jakob Kübarsepp

Department of Mechanical and Industrial Engineering, Tallinn University of Technology, Ehitajate tee 5, 19086 Tallinn, Estonia

ABSTRACT

The evolution of titanium carbonitride (Ti(C,N))-based cermets has seen a notable shift towards environmentally sustainable compositions, particularly through the use of green iron (Fe) binders as alternatives to traditional nickel (Ni) or cobalt (Co) binders, for applications in wear- and corrosion-resistant tooling, such as in oil and gas, chemical processing, and marine environments. A key challenge with Fe-bonded cermets is their limited wear and corrosion resistance. This study investigates the effect of varying chromium (Cr) concentrations (20, 30, and 40 binder wt%) on the microstructural evolution, phase composition, and mechanical properties of Fe-bonded Ti(C,N)-based cermets. Scanning electron microscopy (SEM) and energy-dispersive X-ray spectroscopy (EDS) analyses reveal well-defined core-rim structures and Cr segregation, with increasing Cr content. Grain size increases from 2.03 µm to 2.75 µm, while ceramic phase contiguity rises from 0.61 to 0.80, with higher Cr content. X-ray diffraction (XRD) confirms the presence of Ti(C,N) and Cr-rich Cr_7C_3 carbides, contributing to enhanced hardness of up to 1608 HV through solid solution strengthening and carbide precipitation. However, fracture toughness decreases from 11.55 to 7.82 MPa·$m^{1/2}$ due to increased ceramic connectivity and Cr carbide-induced brittleness. The findings of this study provide valuable insights into optimizing Cr concentration in Fe-bonded Ti(C,N)-based cermets, balancing hardness and toughness to enhance their wear and corrosion resistance. This optimization is crucial for developing durable, environmentally sustainable cermet materials suitable for demanding industrial applications.

1. Introduction

Iron (Fe)-bonded cermets have garnered significant attention in materials science to meet the sustainable development goals of inclusive and sustainable industrialization. Traditionally, cermets have utilized binders such as nickel (Ni) or cobalt (Co); however, the rising costs and health concerns associated with these metals have prompted a shift towards Fe-based binders [1]. Conversely, a critical challenge in the development of iron-bonded cermets is enhancing corrosion and wear resistance. Chromium (Cr) has been identified as a beneficial alloying element in this context. Its addition leads to the formation of stable Cr-rich oxide layers on the material's surface, which act as protective barriers against corrosive agents [2]. Moreover, Cr can form complex carbides, such as $(Cr,Fe)_7C_3$, which contribute to the hardness and wear resistance of the cermets [3,4]. This makes Cr-containing cermets highly suitable for applications in wear- and corrosion-resistant tooling. However, the quantity, distribution, and morphology of secondary chromium carbides can influence the wear and corrosion resistance and the fracture toughness of the composite [5,6].

Despite its advantages, limited research has been conducted on high-Cr-content Fe-bonded Ti(C,N)-based cermets, leaving the optimal concentration largely unexplored. In this study, we systematically investigate the effects of varying Cr concentrations on the microstructure and mechanical properties of Fe-bonded cermets. By analyzing the microstructural evolution, phase composition, and performance metrics, such as hardness and fracture toughness, we aim to elucidate the role of Cr in optimizing the properties of these composites for advanced engineering applications.

2. Experimental procedure

The Ti(C,N)-FeCr cermets were synthesized in a ratio of 70 wt% ceramic to 30 wt% metal, with the binder phase containing high Cr contents of 20 wt%, 30 wt%, and 40 wt%. The powders were first homogenized using planetary ball milling for 72 hours with a ball-to-powder ratio of 10:1 in an isopropanol medium. After milling, the powders were compacted via uniaxial pressing at 200 MPa. The green bodies then underwent sintering at 1550 °C. Post-processing involved cutting samples with a diamond cutting disc, mounting the cross-sections in epoxy resin, polishing the samples up to 0.3 μm with diamond paste, and the final finishing with colloidal silica for a high-quality, visibly pore- and scratch-free surface.

Microstructural characterization was conducted using scanning electron microscopy (SEM) coupled with energy-dispersive X-ray spectroscopy (EDS). Phase transformations of the sintered samples were analyzed using X-ray diffractometry (XRD) with Cu-Kα radiation. The Vickers hardness (HV30) was measured with a load of 30 kgf and a dwell time of 10 seconds, while the fracture toughness (K_{IC}) was determined using the equation proposed by Shetty et al. [7].

3. Results and discussion

3.1. SEM and EDS analyses

Detailed SEM micrographs and EDS elemental compositions presented in Fig. 1 highlight the microstructural characteristics of Ti(C,N)-FeCr cermets at varying Cr concentrations. At 20 wt% Cr, the core-rim structure was well defined, with relatively thin rims of Ti(C,N) and with minimal Cr content (1.01 wt%), indicating more Cr diffusion into the binder phase (6.24 wt%). The microstructure exhibited a relatively homogeneous distribution of binder with fine grains and minimal secondary phase precipitation. The Fe content was predominant in the binder phase, with a highly uniform Cr distribution and minimal segregation. Chromium carbide formation was significantly low (32.67 wt%), with only fine, dispersed carbides present, primarily at grain boundaries.

At 30 wt% Cr addition, the rims were more prominent, showing clear grain growth with a relatively higher Cr content (1.21 wt%). This indicated reduced Cr diffusion into the binder phase (5.48 wt%). The cermet displayed a moderately refined microstructure with a higher density of secondary carbide precipitates. The binder phase became more fragmented due to the Cr-induced formation of secondary carbides (42.24 wt%) along grain boundaries and the areas connecting the grains.

In the 40 wt% Cr cermet, the core-rim structure was significantly developed, with thick Cr-rich rims (2.36 wt%), leading to the formation of complex (Ti,Cr)(C,N) solid solutions along the grain boundaries. The microstructure became coarser due to grain growth driven by higher Cr content, and the binder phase appeared discontinuous due to the extensive formation of Cr-based secondary carbides (45.24 wt%) along the grain boundaries and within the matrix.

3.2. Grain size and contiguity

The binder distribution in Ti(C,N)-FeCr cermets appeared to become more uniform with increasing Cr concentration. The microstructural analysis revealed distinct trends in grain size evolution and ceramic phase contiguity.

The average grain size of the ceramic phase demonstrated a progressive increase with the rise in Cr content (Fig. 2). At 20 wt% Cr concentration, the average grain size was measured at 2.03 μm. Significant grain growth was observed

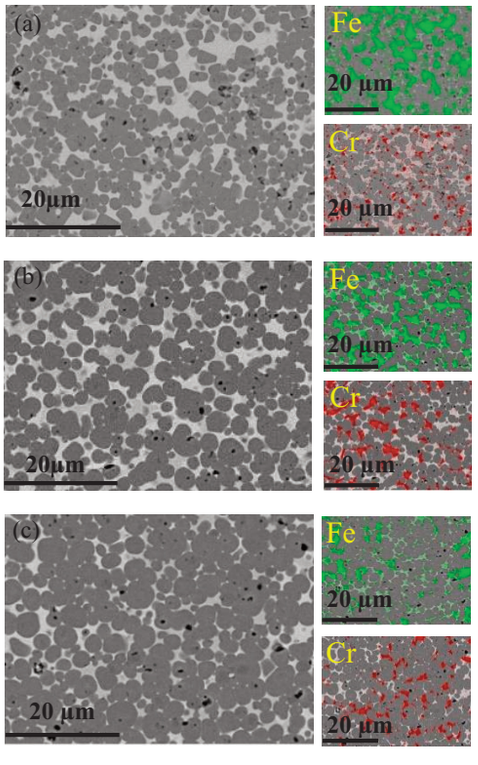

20 wt% Cr	Chemical composition (wt%)					
	C	N	Ti	Cr	Fe	W
Total	7.98	7.12	55.19	5.45	21.82	2.44
Binder	8.14	0.17	3.73	6.24	79.15	2.56
Carbide	10.84	2.31	13.71	32.67	36.69	3.78
Outer rim	10.59	8.32	77.01	1.01	1.10	1.98

30 wt% Cr	Chemical composition (wt%)					
	C	N	Ti	Cr	Fe	W
Total	9.06	4.59	58.76	7.22	18.13	2.26
Binder	7.68	0.19	10.09	5.48	74.59	1.97
Carbide	12.37	0.01	7.09	42.24	36.26	2.03
Outer rim	11.09	5.91	78.79	1.21	1.10	1.90

40 wt% Cr	Chemical composition (wt%)					
	C	N	Ti	Cr	Fe	W
Total	9.35	4.06	64.09	7.80	11.98	2.72
Binder	4.57	0.03	8.76	5.26	79.13	2.25
Carbide	10.70	0.04	9.76	45.24	32.91	1.35
Outer rim	9.73	5.15	79.19	2.36	0.81	2.76

Fig. 1. SEM micrographs with the corresponding EDS elemental mapping and EDS elemental compositions of Ti(C,N)-FeCr cermets with: (a) 20 binder wt% Cr, (b) 30 binder wt% Cr, and (c) 40 binder wt% Cr.

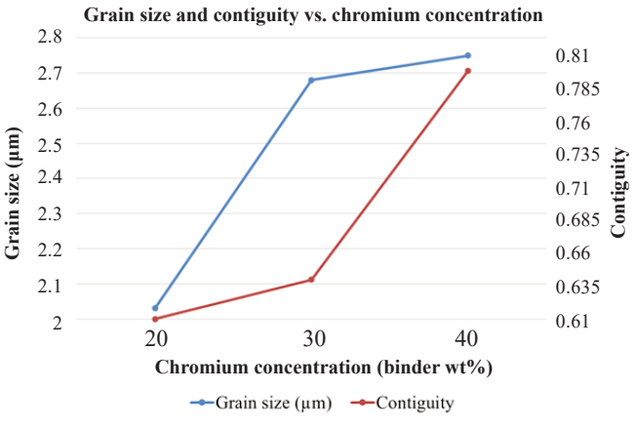

Fig. 2. Grain size and contiguity of Ti(C,N)-based cermets with varying chromium concentrations.

when the Cr concentration increased from 20 wt% to 30 wt%, with the grain size rising to 2.68 µm. This grain growth may be attributed to the enhanced diffusion rates facilitated by Cr, which lowers the grain boundary energy. However, as the Cr content further increased from 30 wt% to 40 wt%, the grain size grew at a relatively reduced rate compared to the previous increment, reaching 2.75 µm. This suggests a saturation effect where the grain growth mechanism becomes less responsive to additional Cr addition. Importantly, the observed grain growth is not substantial enough to adversely affect the mechanical properties.

The contiguity, defined as the fraction of the total grain boundary length shared between ceramic grains, showed contrasting trends compared to grain size evolution (Fig. 2). At 20 wt% Cr concentration, the contiguity was measured at 0.61. Between 20 wt% and 30 wt% Cr concentration, there was a slight increase in ceramic-to-ceramic contact, with contiguity reaching 0.64, indicating a stable phase distribution without significant changes in the connectivity of ceramic grains. In contrast, a substantial increase in contiguity was observed when the Cr content rose from 30 wt% to 40 wt%, with the contiguity sharply rising to 0.80. This marked enhancement suggests improved ceramic network formation, which could be attributed to changes in the binder phase distribution and the corresponding reduction in binder phase continuity.

3.3. Phase analysis

The XRD analysis of Ti(C,N)-FeCr cermets with 20 wt%, 30 wt%, and 40 wt% Cr additions revealed slight variations in phase composition and carbide formation influenced by the increasing Cr content (Fig. 3). Prominent diffraction peaks corresponding to Ti(C,N) were observed in all samples, indicating its dominance as the primary ceramic phase. At 20 wt% Cr, sharp Ti(C,N) peaks with minor signals from Cr-rich carbides, mainly Cr_7C_3, suggested limited solid solution formation, with Cr_7C_3 carbide concentration measured at 7.4%. With 30 wt% Cr, the intensity of Cr-rich carbide peaks increased, with Cr_7C_3 concentration rising to 12.9%. At 40 wt% Cr, a significant increase in the intensity of Cr-rich carbide phases confirmed extensive carbide formation, with Cr_7C_3 concentration reaching 29.6%. The reduction in binder phase peak intensity with higher Cr content suggested improved ceramic phase continuity, correlating with the observed increase in contiguity and grain growth in the microstructural analysis. These findings highlight the role of Cr in promoting solid solution strengthening and enhancing the ceramic network structure in Ti(C,N)-FeCr cermets.

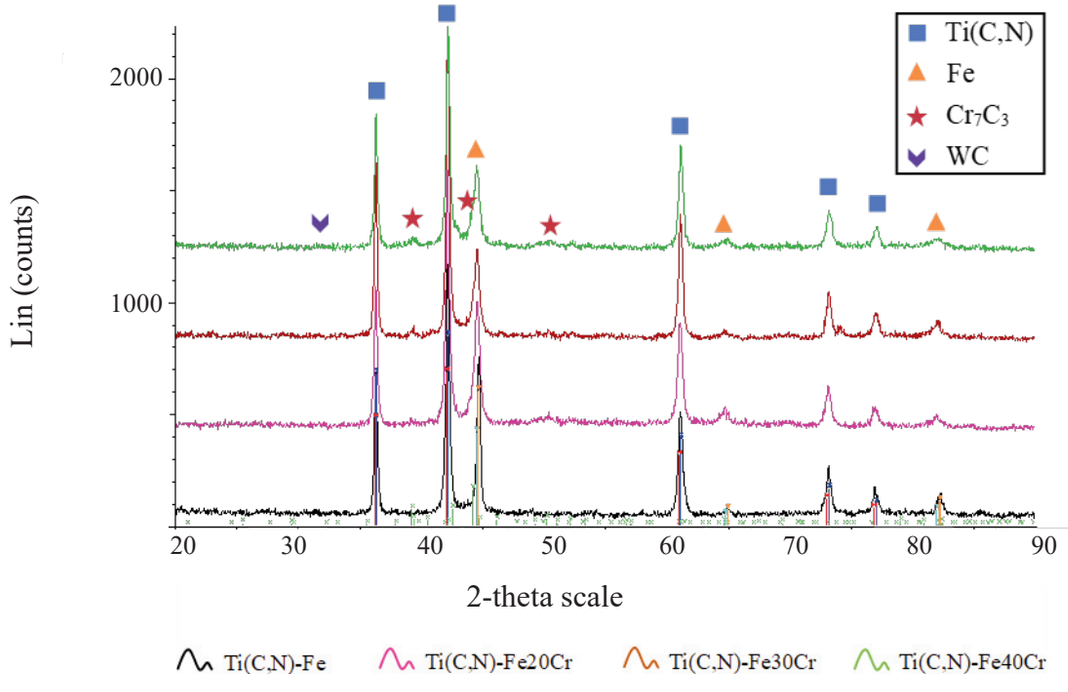

Fig. 3. XRD patterns of Cr-added Ti(C,N)-FeCr cermets at different Cr concentrations.

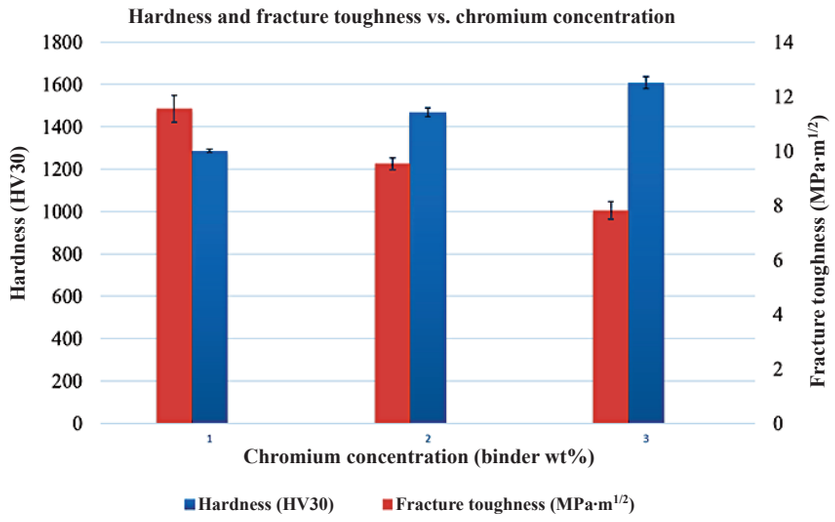

Fig. 4. Hardness and fracture toughness of Ti(C,N)-FeCr cermets as a function of Cr concentration.

3.4. Mechanical properties

The mechanical properties of Ti(C,N)-FeCr cermets, particularly hardness and fracture toughness, exhibited notable trends with increasing Cr content (Fig. 4), which can be directly correlated to the observed microstructural and phase evolution. Hardness measurements revealed a progressive increase with higher Cr additions, rising from 1286 HV at 20 wt% Cr to 1468 HV at 30 wt% Cr, and reaching 1608 HV at 40 wt% Cr. This increase is primarily attributed to the enhanced formation of Cr-rich carbides, particularly Cr_7C_3, which strengthen the ceramic matrix by impeding dislocation motion [8]. Additionally, the progressive thickening of Cr-rich rims in the core-rim structure, as observed in SEM micrographs, contributes to solid solution strengthening. At 40 wt% Cr, a higher degree of ceramic phase contiguity further enhances the material's hardness, resulting in a more rigid but brittle structure.

Conversely, fracture toughness showed a decreasing trend with increasing Cr content, dropping from 11.55 MPa·m$^{1/2}$ at 20 wt% Cr to 9.53 MPa·m$^{1/2}$ at 30 wt% Cr, and further to 7.82 MPa·m$^{1/2}$ at 40 wt% Cr. This reduction in fracture toughness is primarily due to the increased ceramic phase contiguity and reduced binder phase continuity. At 20 wt% Cr, the binder phase is relatively well distributed, facilitating crack deflection and energy dissipation, thereby maintaining toughness. However, as Cr content increases, the binder phase becomes more fragmented and less continuous, as seen in EDS analyses, leading to a reduction in its crack-bridging ability. The formation of a more interconnected ceramic network with thicker Cr-rich rims at 30 wt% and 40 wt% Cr results in brittle fracture pathways, further lowering toughness. Moreover, the increased presence of Cr_7C_3 carbides at higher Cr levels introduces brittle phases that serve as crack initiation sites, intensifying the loss of fracture resistance.

XRD analysis also supports this trend, showing a reduction in binder phase intensity at higher Cr concentrations, indicating a shift toward a more ceramic-dominant structure. The diminished ductile binder phase, combined with enhanced ceramic connectivity and secondary carbide precipitation, significantly restricts crack-bridging mechanisms, making the material more prone to brittle failure.

To achieve an optimal balance, the hardness of low-chromium content cermets can be enhanced through the addition of secondary carbides [8], while the toughness of high-Cr cermets can be improved by increasing the binder phase [10] or incorporating additional metallic elements [11]. Our future research will be dedicated to refining this balance to optimize performance.

4. Conclusions

This study investigated the influence of high chromium concentrations (20 wt%, 30 wt%, and 40 wt%) on the microstructural evolution, phase composition, and mechanical properties of iron-bonded Ti(C,N)-based cermets.

- SEM and EDS analyses revealed a more uniform binder distribution and an enhanced rim phase with increasing Cr content. EDS mapping confirmed that the increase in Cr concentration leads to a less uniform Cr distribution with an increase in Cr segregation at the core-rim interfaces and within the binder phase, promoting the formation of Cr-rich carbides.
- Grain size exhibited a notable increase from 2.03 µm at 20 wt% Cr to 2.75 µm at 40 wt% Cr, with the most pronounced growth occurring between 20 wt% and 30 wt% Cr. Concurrently, ceramic phase contiguity rose markedly from 0.61 to 0.80, particularly between 30 wt% and 40 wt% Cr, indicating enhanced ceramic-to-ceramic connectivity and reduced binder phase continuity.
- Phase analysis via XRD confirmed the presence of Ti(C,N) and Cr-rich carbides (especially Cr_7C_3). The Cr_7C_3 carbide content increased from 7.4% at 20 wt% Cr to 29.6% at 40 wt% Cr, contributing to greater phase stability and hardness through solid solution strengthening and carbide precipitation.
- Mechanically, hardness improved progressively with Cr content, reaching 1608 HV at 40 wt% Cr, driven by solid solution strengthening, carbide formation, and increased ceramic phase contiguity. Conversely, fracture toughness decreased from 11.55 MPa·m$^{1/2}$ at 20 wt% Cr to 7.82 MPa·m$^{1/2}$ at 40 wt% Cr, primarily due to the brittleness of Cr-rich carbides and the dominance of ceramic-to-ceramic contact,

which reduced the energy-dissipating role of the binder phase.

- Overall, while higher Cr content enhances hardness and microstructural uniformity, it compromises fracture toughness, Cr distribution, and binder phase continuity. Therefore, optimizing Cr concentration is critical to achieving a balanced combination of hardness and toughness for superior mechanical performance in Fe-bonded Ti(C,N)-based cermets.

Data availability statement

All research data are contained within the article and can be shared upon request from the authors.

Acknowledgments

This work was supported by the Estonian Research Council grant PRG1145. The publication costs of this article were partially covered by the Estonian Academy of Sciences.

References

1. Kolnes, M., Pirso, J., Kübarsepp, J., Viljus, M. and Traksmaa, R. Structure formation and characteristics of chromium carbide–iron–titanium cermets. *Proc. Estonian Acad. Sci.*, 2016, **65**(2), 138–143. https://doi.org/10.3176/proc.2016.2.09
2. Cintho, O. M., Favilla, E. A. P. and Capocchi, J. D. T. Mechanical–thermal synthesis of chromium carbides. *J. Alloys Compd.*, 2007, **439**(1–2), 189–195. https://doi.org/10.1016/j.jallcom.2006.03.102
3. Pirso, J., Viljus, M., Letunovits, S. and Juhani, K. Reactive carburizing sintering – a novel production method for high quality chromium carbide-nickel cermets. *Int. J. Refract. Met. Hard Mater.*, 2006, **24**(3), 263–270. https://doi.org/10.1016/j.ijrmhm.2005.06.002
4. Kolnes, M., Kübarsepp, J., Kollo, L. and Viljus, M. Characterization of TiC-FeCrMn cermets produced by powder metallurgy method. *Medžiagotyra*, 2015, **21**(3), 353–357. https://doi.org/10.5755/j01.ms.21.3.7364
5. Dong, G., Xiong, J., Yang, M., Guo, Z. and Wan, W. Effect of Mo2C on erosion–corrosion resistance behavior of Ti(C, N)-based cermets. *Wear*, 2012, **294**–**295**, 364–369. https://doi.org/10.1016/J.WEAR.2012.05.013
6. Hussainova, I., Kubarsepp, J. and Pirso, J. Mechanical properties and features of erosion of cermets. *Wear*, 2001, **250**(1–12), 818–825. https://doi.org/10.1016/S0043-1648(01)00737-2
7. Shetty, D. K., Wright, I. G., Mincer, P. N. and Clauer, A. H. Indentation fracture of WC–Co cermets. *J. Mater. Sci*., 1985, **20**, 1873–1882. https://doi.org/10.1007/BF00555296
8. Wang, L., Cao, Z., Jin, N. and Liu, Y. Achieving hardness-strength-toughness synergy in (Ti, W, Mo, Cr)(C, N)-based cermets. *J. Am. Ceram. Soc.*, 2024, **107**(9), 5939–5953. https://doi.org/10.1111/JACE.19870
9. Chicardi, E., Torres, Y., Córdoba, J. M., Hvizdoš, P. and Gotor, F. J. Effect of tantalum content on the microstructure and mechanical behavior of cermets based on $(Ti_xTa_{1-x})(C_{0.5}N_{0.5})$ solid solutions. *Mater. Des.*, 2014, **53**, 435–444. http://doi.org/10.1016/j.matdes.2013.07.039
10. Xu, Q., Ai, X., Zhao, J., Gong, F., Pang, J. and Wang, Y. Effects of metal binder on the microstructure and mechanical properties of Ti(C,N)-based cermets. *J. Alloys Compd.*, 2015, **644**, 663–672. https://doi.org/10.1016/J.JALLCOM.2015.05.059
11. Zhu, G., Liu, Y. and Ye, J. Influence of Ce–Co pre-alloyed powder addition on the microstructure and mechanical properties of Ti(C, N)-based cermets. *Int. J. Refract. Met. Hard Mater.*, 2013, **37**, 134–141. https://doi.org/10.1016/j.ijrmhm.2012.11.008

Suure kroomisisalduse mõju rauapõhise sideainega Ti(C,N) kermistele: kõvaduse ja sitkuse kompromiss

Tabeen Halawat Pampori, Märt Kolnes, Kristjan Juhani, Marek Tarraste ja Jakob Kübarsepp

Titaankarbonitriidsete (Ti(C,N)) kermiste arendamine võimaldab märgatavat edasiminekut jätkusuutlikumate ja keskkonnasõbralikumate komposiitmaterjalide kasutuselevõtul, eriti juhul kui traditsioonilised nikli- ja koobaltipõhised sideained asendatakse „rohelisteks" peetavate rauapõhiste sideainetega, näiteks kulumis- ja korrosioonikindlust nõudvates tööriistades. Rauapõhiste sideainetega kermiste põhiprobleem on seni olnud nende piiratud kulumis- ja korrosioonikindlus. Töös uuritakse kroomisisalduse (20%, 30% ja 40% sideaines) mõju rauapõhise sideainega Ti(C,N) kermiste mikrostruktuurile, faasilisele koostisele ja mehaanilistele omadustele. SEM- ja EDS-analüüsid tõid esile karbonitriidile iseloomuliku rõngassüdamik-struktuuri ning näitasid, et kroomisisalduse suurenemine põhjustab kroomi segregatsiooni. Kroomisisalduse suurenedes kasvab karbiiditera suurus 2,03–2,75 µm-ni. XRD-uuringud tõestasid lisaks titaankarbonitriidile ka kroomirikaste Cr_7C_3-karbiidide esinemist mikrostruktuuris, mis suurendas küll kõvadust (kuni 1608 HV), kuid vähendas samal ajal purunemissitkust (11,55–7,82 $MPa \cdot m^{1/2}$) kroomkarbiidide hapruse tõttu. Töö tulemused pakuvad väärtuslikku teavet kroomisisalduse optimeerimiseks rauapõhiste sideainetega titaankarbonitriidsetes kermistes, suurendamaks nende kulumis- ja korrosioonikindlust. Uurimus on oluline samm vastupidavate ja keskkonnasõbralike kermiste arendamisel nõudlike tööstuslike rakenduste tarvis.